The 14th International Topical Meeting on Nuclear Reactor Thermal Hydraulics (NURETH-14)
Hilton Toronto Hotel, Toronto, Ontario, Canada, September 25-29, 2011.

NURETH14-365

# Flow Induced Vibration Forces on a Fuel Rod by LES CFD Analysis

A. M. Elmahdi[1], R. Lu[1], M. E. Conner[1], Z. Karoutas[1], E. Baglietto[2]
[1]Westinghouse Electric Company LLC, Columbia, SC, USA
[2]CD-adapco, Melville, NY, USA
mandoua@westinghouse.com

## Abstract

The purpose of the present study is to evaluate the feasibility of use of CFD Large Eddy Simulation (LES) modeling techniques in CD-adapco CFD code STAR-CCM+ to calculate the instantaneous stress tensor on the fuel rod wall and then utilize these data for mechanical calculations. Transient hydraulic forces on the fuel rod resulting from the CFD model are linked to the Westinghouse VITRAN code to predict fuel rod vibration response. The coupled CFD/mechanical solution has provided a reasonable prediction of fuel rod vibration and a more accurate representation of all the important physics and excitation forces.

## Introduction

Vibrations of fuel rods caused by turbulence and lateral velocities in PWR reactors is the main cause of Grid to Rod Fretting wear (GTRF) of nuclear fuel assemblies. Developing calculation methods and codes for prediction of GTRF has been a challenging task. It is not yet possible to completely characterize by computer simulations the vibration and fretting behavior of a fuel rod, taking into account simultaneously the turbulent axial flow along the rod and the larger scales of the flow, including non-axial flow around fuel rods.

The work presented in this paper is part of a large program to develop a complete analytical methodology for prediction of GTRF in fuel assemblies. VITRAN (VIbration TRansient Analysis – Nonlinear) is a special code developed by Westinghouse to simulate flow induced vibration and fretting wear of a fuel rod [1 and 2]. VITRAN is a non-linear dynamic model of a nuclear fuel rod and its supports developed and integrated to a fretting-wear analysis method to predict the performance of fuel assemblies. VITRAN calculates the rod frequency response and motion, the support impact forces (normal and friction forces), the sliding and sticking distances and the work rates [1 and 2].

This paper presents the computational Fluid Dynamic (CFD) modeling methodology used to predict the transient forces on fuel rod and the validation of CFD solution. The CFD modeling methodology for prediction of the transient forces on fuel rods was developed using the STAR-CCM+ CFD code. The methodology was validated by benchmarking CFD results versus small-scale experiment.

## 1. CFD analysis

Fuel assemblies are typically built from square arrays of 14x14, 15x15, 16x16 or 17x17 fuel rods. Fuel rod diameters vary from 0.360 inch (9.144 mm) to less than 12.7 mm and are typically longer than four meters. These fuel rods are held together by structural grids which

provide the mechanical support to the rods. For most of Westinghouse fuel designs, the mixing vanes on the top of the grid straps are used to increase flow mixing and turbulence to enhance the heat transfer and DNB (Departure from Nucleate Boiling) margin. However, these mixing vanes increase turbulence and vibration forces on fuel rods.

Hydraulic testing is important in understanding critical parameters which may cause the rod to vibrate such as hydraulic forces on fuel rod. Current hydraulic testing can only provide limited information at specific locations on a fuel rod where the instrumentation is placed and only provide the vibration response. Therefore, complete resolution of the forces on fuel rods is only possible through use of Computational Fluid Dynamics (CFD).

### 1.1 CFD solution method

CFD based on RANS modeling has been used by Westinghouse Nuclear Fuel for modeling and predicting single-phase flow conditions downstream of structural grids that have mixing devices [3]. While steady state CFD methodology for solution of the flow fields downstream mixing vane grids was validated using data from experimental testing [3], forces on fuel rods for mechanical analysis require transient CFD solution.

A transient CFD computer simulation of a complete fuel assembly would require a large amount of computing power, time and memory which is essentially very difficult if not possible with the current state of computers. There is hence a need to determine by simplified smaller models the vibration forces on a fuel rod. The geometry used in the CFD analysis is shown in Figure 1.

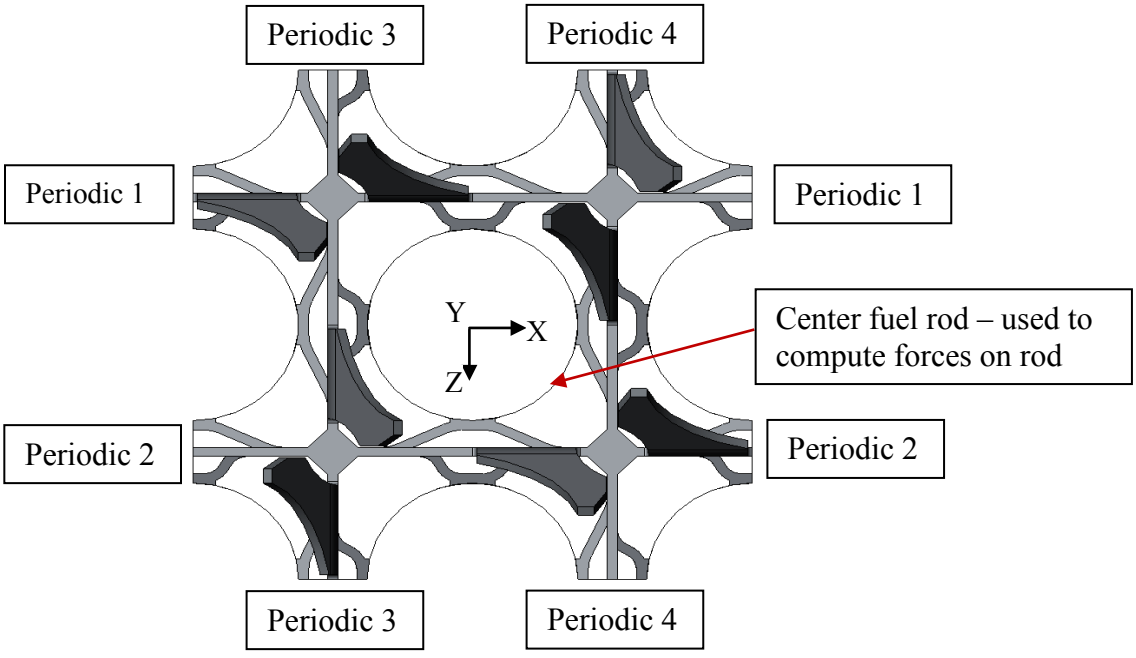


Figure 1: Grid Geometry and Periodic Boundary Conditions Used in the CFD Model

The dominant frequencies of vibration of fuel rods are less than 100 Hz [4]. Therefore, Large Eddy Simulation (LES) computation method is appropriate for this application. The LES with the Wale subgrid model available in STAR-CCM+ was used in the CFD solution.

The LES solver of STAR-CCM+ has been previously validated on fundamental flow cases, and recently excellent predictions have been demonstrated on the OECD/NEA benchmark experiments [5]. The present simulations adopt the same approach used in the OECD/NEA benchmark, which adopts the WALE subgrid model, in combination with bounded central differencing scheme for spatial discretization of the momentum equations and a blending factor of 0.1. A second order implicit formulation is employed for temporal discretization and the physical time-step is chosen in order to produce an average Courant number of around 1.

As the target of the present work is to develop a practical approach for analysis of flow induced vibrations, a concern is the near wall requirements of LES, for this reason in the present work the LES simulations are not resolved at the wall but they are instead coupled to classic wall functions. The rationale behind this approach is related to the particular configuration of the flow, where due to the extremely narrow flow passages and complexity of the spacers practically all the turbulence of interest is generated by the spacer obstruction rather than the wall shear. Jayaraju [5] has shown how for this kind of flow configurations resolved and unresolved near wall LES predict practically identical flow fields.

Reynolds number in PWR reactors is around half a million based on fuel assembly flow area, however, most of experiments used in validation of CFD solutions are done in lower Reynolds number. The Reynolds numbers in the 5x5 test assemblies used in PIV testing described in Section 2 are around 30000 to 40000. Reynolds numbers in the full fuel assembly vibration testing are on the order of 240000 to 250000. Since the results from CFD models are used to calculate the fuel rod vibration responses which are compared to rod vibration responses from experiment, a Reynolds number used in the full scale vibration testing of full fuel assembly is used in the CFD model.

### 1.1.1 Computational geometry and boundary conditions

The 3×3 rod bundle geometry used in the CFD analysis is representative of a 17×17 fuel assembly design. The rod bundle pitch (12.6 mm), rod diameter (9.5 mm), and grid features are identical to a 17×17 fuel assembly. The only reduction in scale is in the overall 3×3 array versus a 17×17 array. The concept grid used in this CFD analysis case is shown in Figure 1. One span is modeled in the CFD model. Figure 2 shows the axial configuration of the CFD model.

Uniform inlet velocity of 5.0 m/sec was applied at the inlet (lower horizontal plane). It is important to note that the use of a simple uniform inlet conditions is justified by the fact that the presence of the spacer is the dominant factor in the turbulent flow configuration as verified in preliminary tests. A comparison between the flat inlet and a more computationally expensive Synthetic Eddy Method [6] available in STAR-CCM+ in fact revealed no appreciable differences in the flow distribution downstream of the spacer. On the other side of the domain (downstream outlet horizontal plane), zero gradient boundary conditions were applied. Since the 3x3 array is a small part of the full grid, periodic boundary conditions were applied. Each opposite vertical

gaps between the fuel rods of the four pairs of the gaps was paired together, see Figure 1. No-slip (zero velocity) boundary conditions were applied on the fuel rods and grid surfaces. Fluid density and viscosity at 250 F is used in the model, same temperature of water in vibration testing.

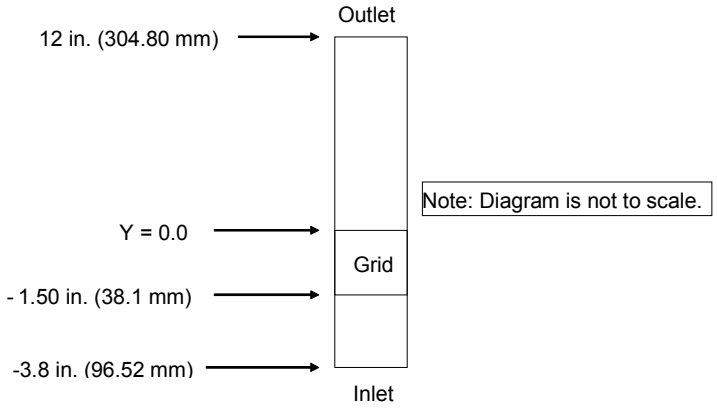


Figure 2: Modeled one span flow domain

### 1.1.2 Mesh generation

The mesh of the model of one span length of the 3×3 nuclear fuel rod bundle, including the very complex grid spacer and mixing vane area, has been created using the STAR-CCM+ code. Figure 3 shows a representative detail of the mesh in the region surrounding the center fuel rod. The core mesh region is composed of uniform cubic hexagonal cells, the grid is consistently refined in proximity to all walls, and multi layer hexagonal cells are adopted in the near wall region and connected to the core grid with the use of trimmed transition elements. The adopted meshing approach allows placing a sufficient number of computational points efficiently, even in complex regions such as the springs of the spacer grid, as shown in Figure 4. The use of flow aligned cubic hexagonal cells has the clear advantage of guaranteeing the grid quality, and eliminating aspect ratio and skeweness issues typical of tetrahedral meshes. In the present work the absolute sizing of the computational cells has been derived from previous mesh convergence studies on a reduced 1 rod configuration, where they have demonstrated the ability of accurately capturing the average and local flow field, furthermore it has also been confirmed that the cell size respect the condition of being less than 1/10 of the RANS predicted integral length scale of turbulence. The total size of the mesh is about 48 Million cells. Mesh size coupled with inlet flow velocity and time step of 5E-5 second resulted in a Courant number of around 1.8 based on inlet velocity. The LES model in STAR-CCM+ is applied in conjunction with a law-of-the wall where the discussed boundary fitted grid construction near the walls, with local control of mesh thickness, results in Y+ values for the first computational points between around 40 and 60.

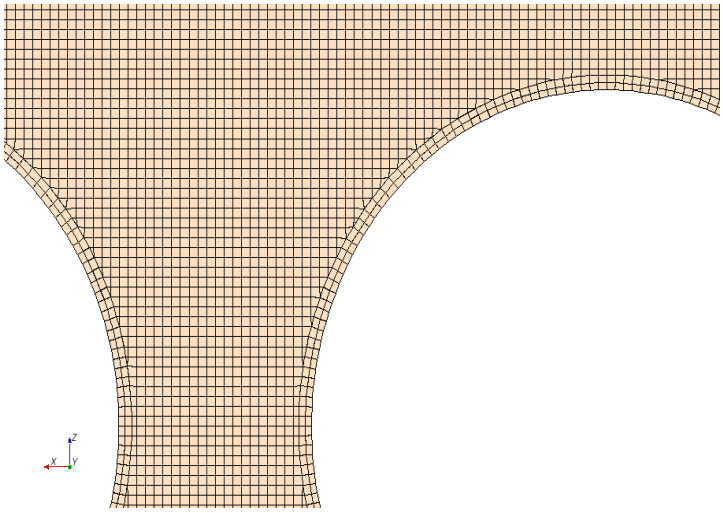

Figure 3: Details of the mesh around the center rod

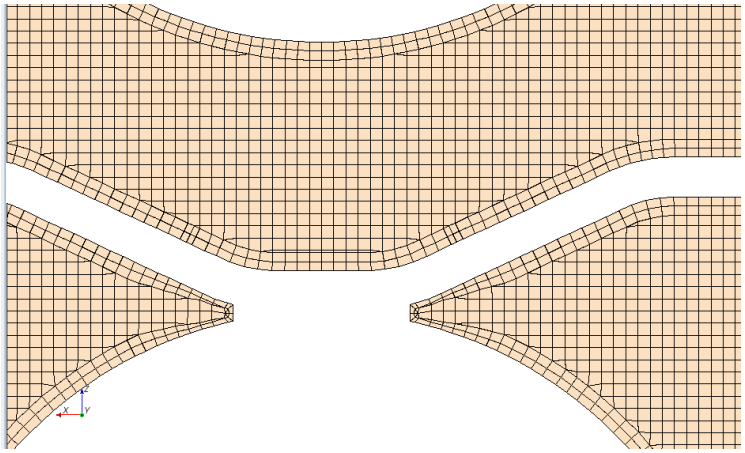

Figure 4: Mesh close to the grid spring

## 2. Validation hydraulic test data

Flowfield velocities obtained from the CFD model were compared to available experimental results from small-scale experiments (i.e., 5×5 rod bundle versus full size 17×17 rod bundle) to benchmark the CFD results.

Particle Image Velocimetry (PIV) is the technique used to measure the lateral flow field velocities. Details of the testing methodology and results are contained in reference [7]. The PIV data is taken at an axial velocity of 2.45 m/s and at ambient temperature resulting in Reynolds number in the range of 30000 to 40000. The lateral velocities measurements were done at different axial locations downstream of the grid so that the lateral velocity development and decay downstream of a grid with mixing vanes can be measured. Multiple velocity fields are averaged to obtain the time-averaged velocity vector fields. This time-averaged velocity vector field is compared against the velocity results from the CFD simulations.

## 3. Results

Two CFD runs were conducted. The geometry shown in Figure 1 is used in the first run. The second run used the same geometry as in Figure 1 after removing the vanes. Boundary conditions used are the same for both models.

To validate the CFD model described in Section 1, comparisons are made between the CFD model results and the experimental data described in Section 2. For this paper, local comparisons of lateral flow field will be provided. Comparison of the transient results from the CFD model to experimental transient results are being developed and will be presented at a future paper. In addition, the mechanical rod response as a result of hydraulic excitation from forces generated from the CFD model is presented and the rod responses are compared to experimental results.

### 3.1 Comparison of CFD results and hydraulic test data

The lateral flow field (perpendicular to the axial flow) at specific elevations from CFD model is compared to the PIV result. Note that the PIV experimental test is conducted at a lower Reynolds number and inlet velocity compared to CFD. Prior studies have shown that the flow structures are independent of temperature and Reynolds number [3]. In this validation case, the CFD code predicts very similar flow field structures to the test data. The lateral velocity magnitude is directly related to the axial velocity so the magnitude of lateral velocity does not match. As the data are compared between CFD and PIV, it is important to note the differences in the two techniques. The PIV data represent an average of 13 instantaneous velocity fields [7]. Since the elevation compared in Figures 5 and 6 is close to the spacer grid, the turbulence in the flow is very high. Therefore, the lateral flow structures, such as the regions of local swirling flow (called vortices in this paper), are not stationary. As a result, an average of instantaneous images will cause these vortices to have lower velocity magnitudes in comparison with the maximum velocity magnitude in a single instantaneous velocity field – i.e., the peak velocity magnitudes are smeared out since the velocity at any one point changes as the swirling flow structure moves.

Figure 5 (a and b) shows the lateral velocity vector from PIV and CFD at an elevation of 17 mm (0.67 in) above the top of the grid strap, downstream from the vane tips. Figure 5 shows swirling flow generated by the vanes clearly. The CFD code predicts the same lateral flow structure as the test data: two vortices in the subchannel center and same flow direction in the gap between the rods. In addition, the CFD model predicts the vortices near the rod gaps (see arrows in Figure 5) that are measured by the PIV technique. At other elevations, the axial development and decay of the vortices is also predicted well by the CFD simulation. Figure 6 (a &b) provide another example.

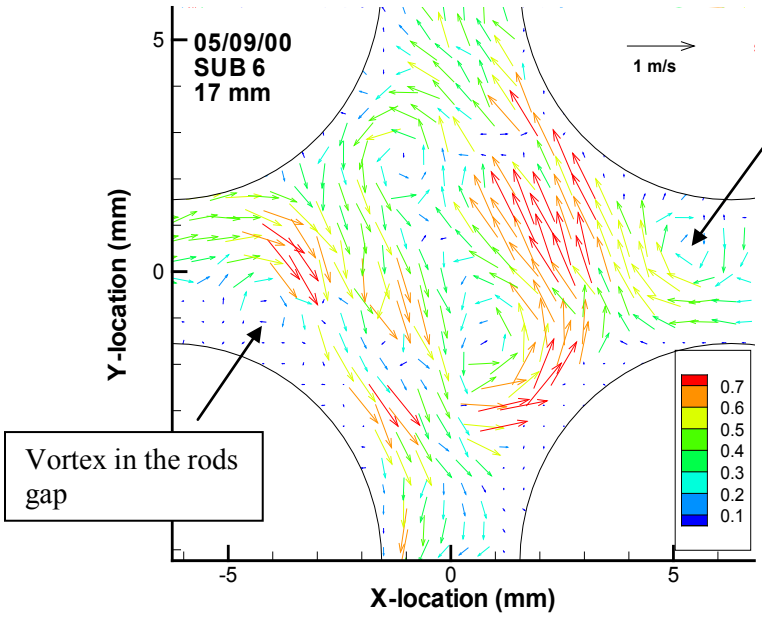


Figure 5 (a) Lateral velocity vectors from PIV data at 0.67 inch above strap

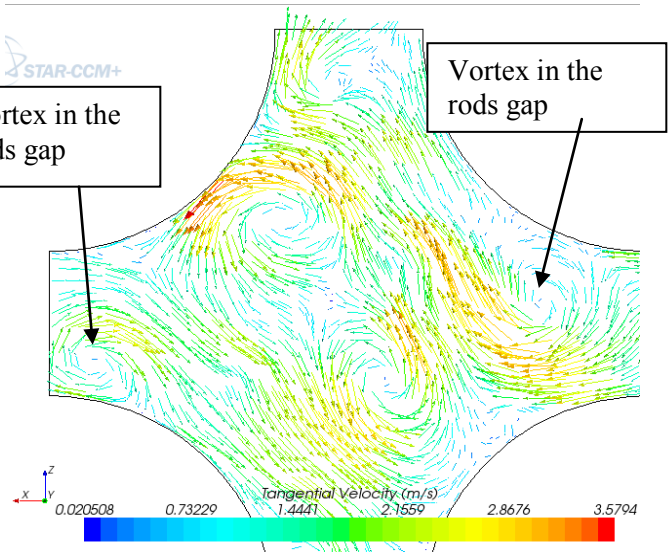


Figure 5 (b): Lateral velocity vectors from CFD at 0.67 inch above strap

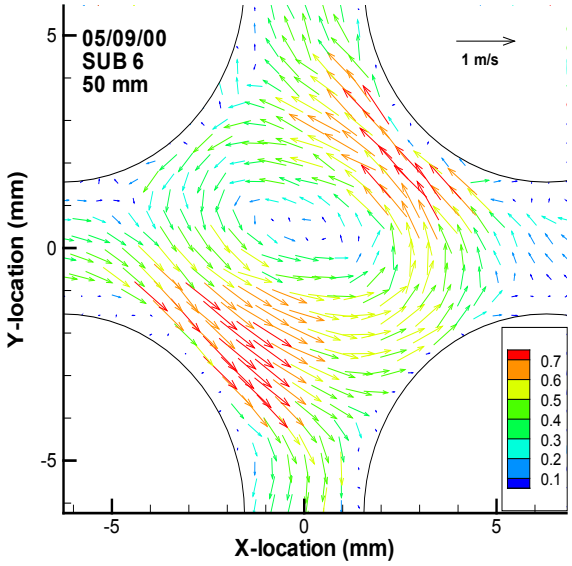


Figure 6 (a) Lateral velocity vectors from PIV at 1.97 inch above grid strap

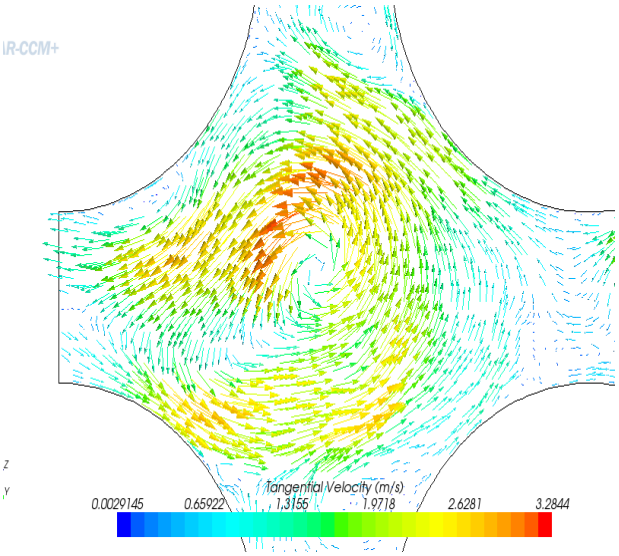


Figure 6 (a) Lateral velocity vectors from CFD at 1.97 inch above grid strap

### 3.2 Rod Mechanical Response

For the purposes of the calculation of the transient forces on the fuel rod, the center rod in the CFD model is used. The fuel rod is divided into segments of 25.4 mm (inch). Transient

forces acting on the fuel rod surface from CFD model are integrated at each rod segment at each time step in two lateral directions, for this analysis the two lateral directions are X and Z directions, see Figure 1. Standard deviations of the force time series are shown in Figures 7 and 8. In vibration terminology, the standard deviation of a fluctuating quantity in time domain is the overall vibration amplitude, RMS. Two observations can be clearly obtained from Figures 7 and 8.

a) Mixing vanes are the main source which generate the excitation forces on fuel rod. The grid with mixing vanes generates much higher turbulence forces compared to the grid without mixing vanes.
b) The excitation forces generated by mixing vanes decay along the span downstream the grid. Both observations are consistent with the results from DNB and heat transfer tests.

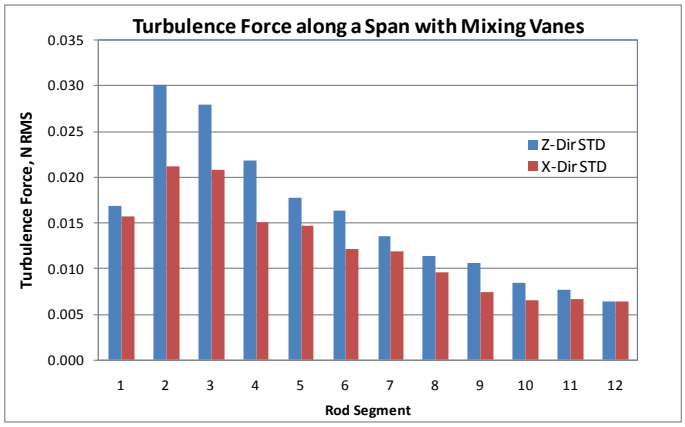


Figure 7: Excitation force distribution along a span – Grid with mixing vanes

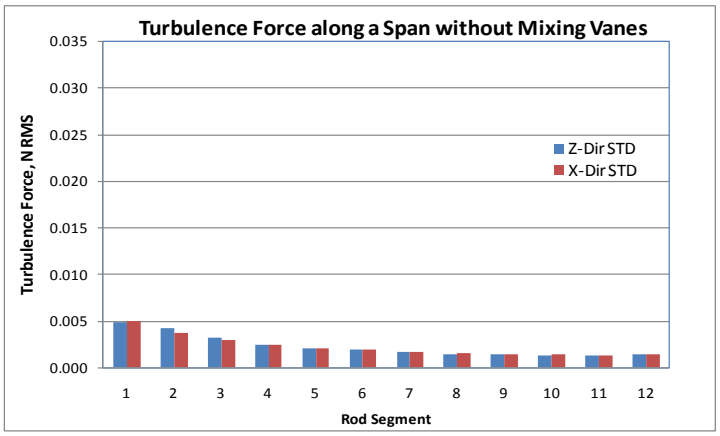


Figure 8: Excitation force distribution along a span – Grid without mixing vanes

The standard deviation of a fluctuating time series data can also be obtained from any Fast Fourier Transform (FFT) analyzer or FFT code as the overall vibration amplitude in RMS. Figure 9 shows a comparison of the two methods. The standard deviation of the transient forces on fuel rods is calculated using Excel spread sheet. FFT analysis results are from a code programmed using MATLAB™. The results are almost identical, see Figure 9. FFT

amplitude and PSD (Power Spectral Density) spectrum plots are shown in Figures 10 and 11. The spectral plots show that the spectrum components of turbulence excitation force are below 200 Hz, which is consistent with the observation by other researchers [8].

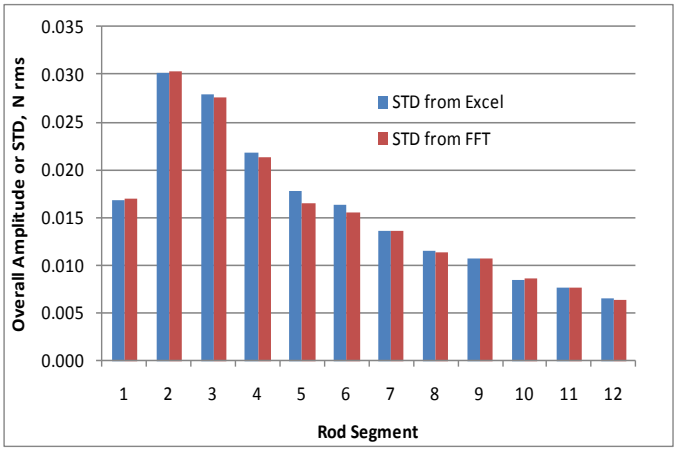


Figure 9: Standard Deviation comparison of Excel and FFT code

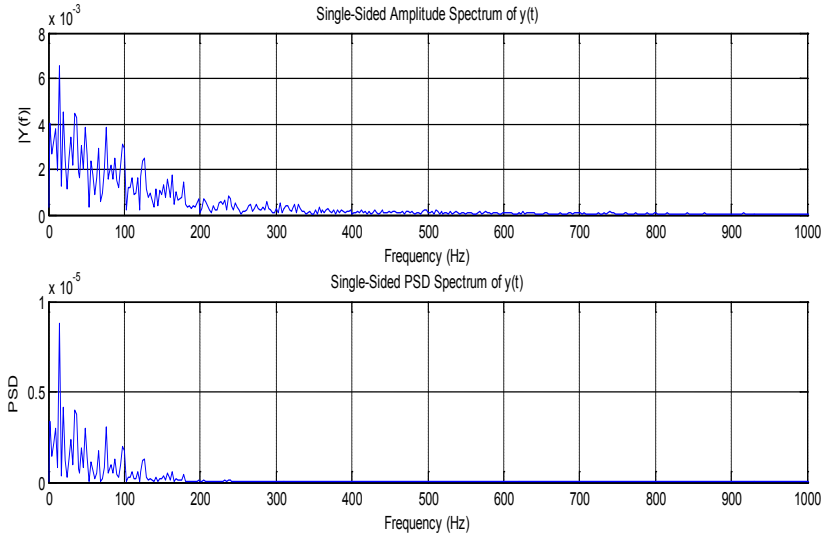


Figure 10: FFT amplitude and PSD spectrum – Segment 2

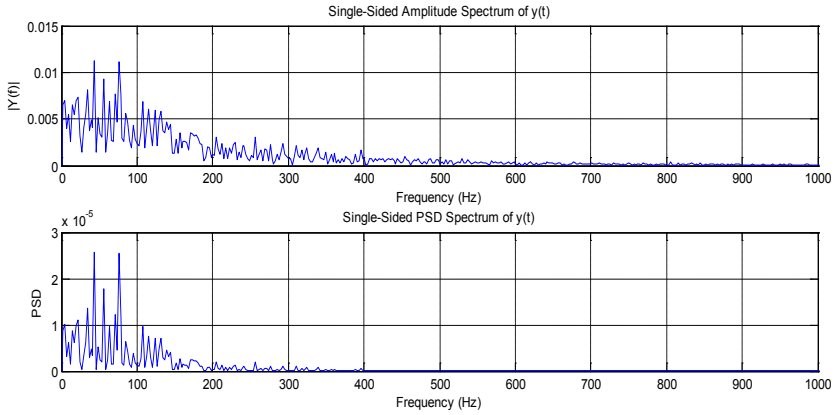


Figure 11: FFT amplitude and PSD spectrum – Segment 7

The other important parameter for applying those excitation forces to fuel rod vibration calculation is the correlation between segment forces. The population correlation coefficient $\rho_{X,Y}$ between two random variables X and Y with expected values $\mu_X$ and $\mu_Y$ and standard deviations $\sigma_X$ and $\sigma_Y$ is defined as:

$$\rho_{X,Y} = corr(X,Y) = \frac{\mathrm{cov}(X,Y)}{\sigma_X \sigma_Y} = \frac{E\left[(X-\mu_X)(Y-\mu_Y)\right]}{\sigma_X \sigma_Y}$$

where E is the expected value operator, cov means covariance, and corr a widely used alternative notation for Pearson's correlation. Table 1 shows some calculation results of the correlation coefficient. The correlation coefficient is symmetric: corr(X,Y) = corr(Y,X). The results show that the correlation between each segment is not strong. Only the adjacent rod segments have some correlations and correlation coefficients vary from 0.11 to 0.44.

| | Z1 | Z2 | Z3 | Z4 | Z5 | Z6 | Z7 | Z8 | Z9 | Z10 | Z11 | Z12 |
|---|---|---|---|---|---|---|---|---|---|---|---|---|
| Z1 | 1.00 | | | | | | | | | | | |
| Z2 | | 1.00 | 0.25 | -0.05 | 0.04 | -0.02 | | | | | | |
| Z3 | | | 1.00 | 0.12 | 0.03 | | | | | | | |
| Z4 | | | | 1.00 | 0.20 | 0.02 | | | | | | |
| Z5 | | | | | 1.00 | 0.11 | 0.18 | 0.03 | | | | |
| Z6 | | | | | | 1.00 | 0.19 | -0.03 | | | | |
| Z7 | | | | | | | 1.00 | 0.30 | 0.17 | | | |
| Z8 | | | | | | | | 1.00 | 0.44 | 0.02 | -0.20 | |
| Z9 | | | | | | | | | 1.00 | 0.20 | -0.07 | |
| Z10 | | | | | | | | | | 1.00 | 0.27 | -0.13 |
| Z11 | | | | | | | | | | | 1.00 | 0.16 |
| Z12 | | | | | | | | | | | | 1.00 |

Table 1: The correlation coefficients of segments

For simplicity, based on the profile of force along span, three lumped forces are used to replace the point forces calculated at every one segment along each span. Each lumped force is the summation of several segment forces (see Figure 12). The lumped forces are located at the elevation of 2 inch, 4.5 inch and 9 inch, respectively. The lumped forces are not correlated to each other.

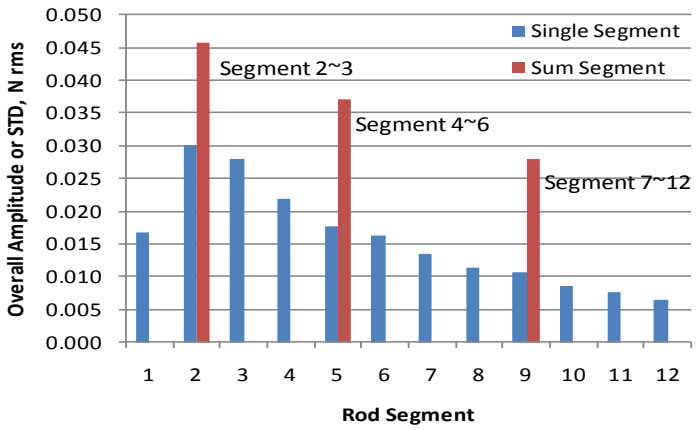


Figure 12: Segment forces and lumped forces

VITRAN (Vibration Transient Analysis Non-linear) is a special code developed by Westinghouse. The code is used to simulate non-linear vibration of a nuclear fuel rod and dynamic interaction between the fuel rod and supports. The code also integrates a fretting-wear (FW) analysis method to predict FW performance [1 and 2]. VITRAN is used in this feasibility study by applying the lumped forces calculated from CFD results to a fuel rod model. Fuel rod model has six support grids. For each span, the three lumped forces shown in Figure 12 were applied. The magnitude of each lumped force is the Standard Deviation (or RMS) of the summation of several segments in time domain. For example, the second lumped force is the summation of Segments 4, 5 and 6. Lumped forces are modeled as white noise random signal with a frequency range from 5 Hz to 100 Hz.

Figures 13 and 14 show the fuel rod vibration amplitude from VITRAN simulations which uses CFD results as input and fuel rod vibration amplitude from testing at similar flow conditions of CFD model with exception of axial input velocity. In general, VITRAN/CFD simulation resulted in higher vibration amplitude compared to test data, however, the results are close.

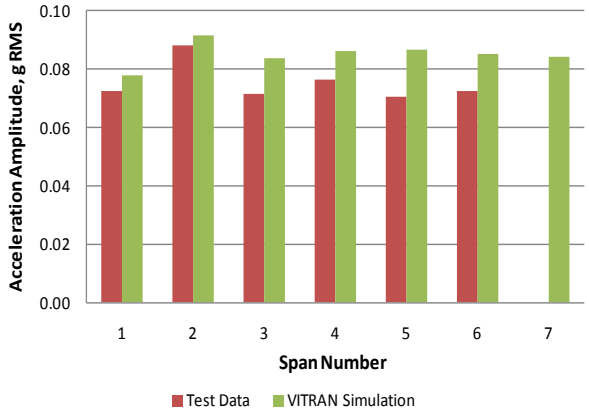


Figure 13: Fuel rod acceleration vibration amplitude: Test data vs. CFD/VITRAN simulation

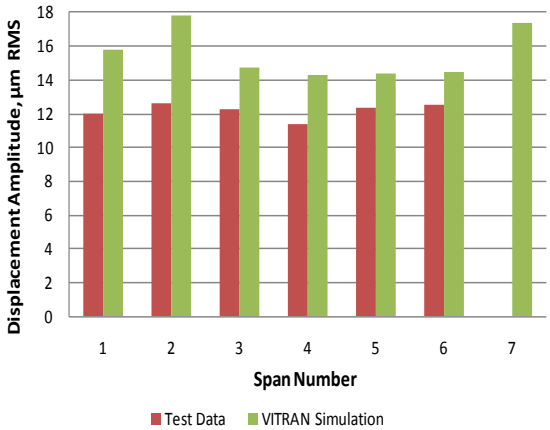


Figure 14: Fuel rod displacement vibration amplitude: Test data vs. CFD/VITRAN simulation

## 4. Conclusions and future work

The work presented in this paper is part of a large program to develop a complete analytical methodology for prediction of GTRF in fuel assemblies. This paper presents the CFD modeling methodology used to predict the transient forces on fuel rod and the validation of CFD solutions. Preliminary hydraulic results from LES CFD model agree well with experimental data. Transient forces on fuel rods predicted by CFD are used as input to the VITRAN code. Results of the rod acceleration and amplitude of vibration calculated by VITAN compared to experimental data are encouraging. Further detailed comparisons of the transient and time averaged CFD results to experimental data are warranted and are underway.

## 5. References

1. P. R. Rubiolo, "Non Linear Fuel Rod Vibration Model: Parametric Studies", Proceedings of the International Meeting on LWR Fuel Performance (TOPFUEL), Orlando, September, 2004.
2. P. R. Rubiolo and M. Y. Young, "VITRAN: An Advance Statistic Tool To Evaluate Fretting-Wear Damage", 15th International Conference on Nuclear Engineering (ICONE15), Nagoya (Japan) April 22-26, 2007.
3. M. E. Conner, E. Baglietto, A. M. Elmahdi, “CFD Methodology and Validation for Single-Phase Flow in PWR Fuel Assemblies,” Nuclear Engineering and Design Journal Topical issue, Experiments and CFD Code Applications to Nuclear Reactor Safety (XCFD4NRS), Volume 240 (9), September 2010.
4. R. Y. Lu, M. E. Conner, M. L. Boone, C. L. Wilbur and R. Marshall “Nuclear Fuel Assembly Flow-Induced Vibration and Endurance Testing”, Proceeding of Symposium on Flow-Induced Vibration – 2001 ASME Pressure Vessels and Piping Conference July 22-26, 2001, Atlanta, Georgia, USA.
5. S.T. Jayaraju, E.M.J. Komen and E. Baglietto. 2010 “Large Eddy Simulations for Thermal Fatigue Predictions in a T-Junction: Wall-Function or Wall-Resolve Based LES,” CFD4NRS-3 Workshop, Bethesda, MD 2010.
6. N. Jarrin, S. Benamadouche, D. Laurence, and R. Prosser. 2006. "A synthetic-eddy-method for generating inflow conditions for large eddy simulations," International Journal of Heat and Fluid Flow, 27, pp. 585-593.
7. H.L. McClusky, M.V. Holloway, D. E. Beasley, M.E. Conner, “Development of Swirling Flow in a Rod Bundle Subchannel”, ASME Journal of Fluids Engineering 124, 747–755.
8. M.K. Au-Yang, Flow-Induced Vibration of Power and Process Plant Components – A Practical Workbook, 2001.